Real-time Implementation of Grid Code Compliant Grid Edge Energy Management System

Faeza Hafiz, Dmitry Ishchenko, Anil Kondabathini,
Ghanshyamsinh Gohil, David Lawrence, Rasik Sarup

***Abstract*—Integrated distributed energy resources (DER) in a distribution system need to follow grid codes to avoid violations that result in DER/circuit segment disconnection. To comply with grid code requirements at the grid edge level, network constrained grid edge energy management system (EMS) can be deployed. The objective of grid edge EMS is to provide economic solution for active and reactive power DER setpoints at each dispatch interval and ensure voltage regulation to support secure interconnection of the grid edge segment to the distribution system with multiple inverter based DER units. In this work, real-time simulation of grid code compliant grid edge EMS is deployed in a realistic feeder circuit segment. For real-time simulation, communication between the grid edge EMS and DERs is done exploiting IEC 61850-7-420. It enables interoperability among different DERs and grid edge EMS. No prior art has deployed IEC 61850-7-420 GOOSE communication protocol for grid edge EMS. Conversion of IEC 61850 GOOSE messages to Modbus communication protocol is also performed to communicate with grid edge EMS in commodity-off the shelf embedded boards in this work. The real-time simulation in OPAL-RT real-time digital simulator shows the out-performance of grid edge EMS by reducing the voltage violation in the distribution circuit.**

***Index Terms*—Energy management system, Energy Storage, Solar Generation.**

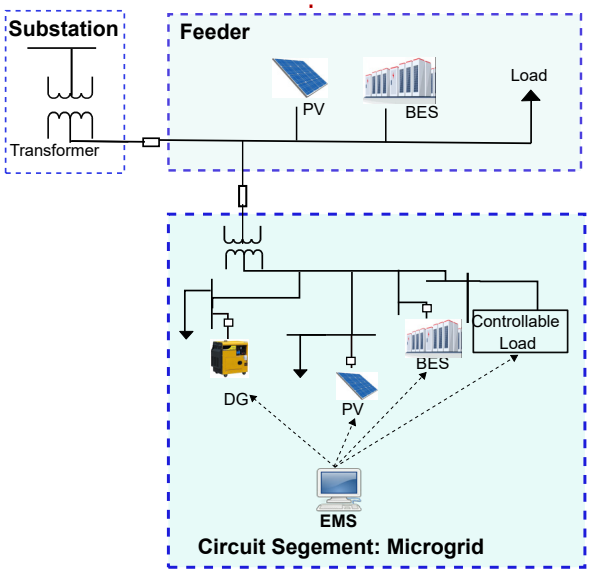

Fig. 1: Circuit segment connected to the grid though a feeder.

I. Introduction

Circuit segments in a distribution system includes different DERs along with several loads. Grid edge technology can be deployed in these segments for decentralization and improving reliability. Loads and energy resources can interact in an intelligent way through grid edge technology. Microgrids can also be considered as grid edge circuit segments when they are connected to the grid. Example of a grid edge circuit segment is shown in Figure 1. A circuit segment can have a grid-edge EMS that dispatches its DERs to minimize its generation costs.

In literature [1], an overview of microgrid EMS function is covered. Some of the works considers grid connected EMS for microgrid where network constraints are not included [2]. On the other hand, network constraints are considered in microgrids when it is in islanding condition [3], [4], [5]. If all the grid connected circuit segments start to operate their DERs without considering the network constraints in EMS, the grid may face instability, especially with the increased penetration of renewable resources. To ensure stable grid operation, circuit segments should operate their DERs in compliance with the grid codes (e. g. IEEE 1547-2018 standard [6]). Impact of network constraints inclusion in EMS of a grid edge circuit segment is shown in our previous work [7]. In [7], steady state load flow is performed in OpenDSS [8], that ensures economic dispatch setpoints are in operating region of voltage defined by IEEE 1547 standard. In this work, network constraint grid edge EMS is deployed in a real-time system to show enhanced integration of the circuit segments into the grid.

For real-time simulation of network constraint grid edge EMS in OPAL-RT, DERs are required to communicate for information exchange. To create a communication and control architecture that can be most widely accepted by the industry (i.e., vendors, distribution system operators (DSOs), aggregators, and other energy service providers), there is a growing need to have an open standard that defines the

communication and control interfaces for all DER devices. IEC 61850 standard with DER model extensions follows this criteria. The advantage of utilization of IEC 61850 standard is to maintain interoperability among various devices by using unified semantic DER models and low-overhead publisher-subscriber communications. In this research, IEC 61850-7-420 Edition 2.0 semantic mode is implemented to establish communication between DERs [9]. No prior art has shown the implementation of IEC 61850 for real-time simulation of grid edge EMS.

IEC 61850-7-420 Edition 2.0 information model is created, mapped to IEC 61850 GOOSE publisher-subscriber messages, and deployed in a real-time system to communicate with DERs and grid edge EMS in this research. Commercial off the shelf boards (Raspberry Pi) are used to be considered as remote terminal units (RTU) for DERs to convert IEC 61850 GOOSE into Modbus protocol to communicate with grid edge EMS. Real-time simulation shows that grid code compliant grid edge EMS maintains voltage through the entire grid edge circuit segment while performing economic dispatch among the existing DERs.

The paper is organized as follows. In Section II, grid code compliant grid edge EMS is described. Real-time simulation set-up is demonstrated in Section III. Simulation results are provided in Section IV. Section V concludes the summary of the work.

II. Grid Edge Energy Management System

The grid edge EMS consists of two parts - solar generation forecasting algorithm and energy management system. These two parts are described in following subsections.

A. Forecasting Algorithm

Energy management system requires forecasting PV generation for the next scheduling interval. Based on the forecasted values, the EMS algorithm is executed, and active and reactive power dispatch commands are sent to the DERs. In grid-edge EMS, long short term memory (LSTM) based deep learning algorithm is leveraged to forecast solar generation. LSTM is one of the recurrent neural network (RNN) structures. LSTM is more powerful compared to the other conventional neural network structures because it consists of a memory cell in its structure to remember the important states in the past and has a forget gate to learn to reset the memory cell for the unimportant features during the learning process. To build up a LSTM model, an input vector is required to provide to the model for predicting the output. The details of LSTM are discussed in [10].

In this work, LSTM models are trained with an input feature vector of 9 features (month stamp, time of the day, solar generation for previous five days at the same time stamp) are utilized to predict the generation for next interval.

B. Energy Management System

Given the DER schedule of the online generators and the energy storage charging/discharging status/rate, the objective of economic dispatch in grid edge EMS is to minimize the operation cost for the present time interval. To avoid violation of the grid code, it also integrates violation constraints. If the energy purchase cost from grid is C_{gd}, from diesel generator (DG) is C_{dg}, weight factor of battery energy storage (BES) device to charge during off-peak hours and discharge during peak hours is w_{es}, then the objective function is

$$min\left(C_{gd}P_{gd} + \sum_{dg=1}^{n_{dg}} C_{dg}P_{dg} + \sum_{es=1}^{n_{es}} w_{es}P_{es}\right) \quad (1)$$

Here, P_{gd} is the electricity purchase from grid, P_{dg} is the purchase from DG, and P_{es} is delivered or absorbed power from BES. If P_{PV} is the solar generation and K is the load loss factor, the power balance equation is

$$P_{gd} + \sum_{dg=1}^{n_{dg}} P_{dg} + \sum_{pv=1}^{n_{pv}} P_{pv} + \sum_{es=1}^{n_{es}} P_{es} = KP_{ld} \quad (2)$$

The BES needs to balance state-of-charge (SOC). Equation for charge balance constraint at time period, t is

$$SOC_{es,t} = SOC_{es,t-1} - \frac{P_{es}\Delta t\eta}{\psi_{es}} \quad (3)$$

Here, η is the charging/discharging efficiency and ψ_{es} is the BES capacity. It also needs to follow maximum and minimum threshold level stated as

$$SOC_{es}^{max} \leq SOC_{es,t} \leq SOC_{es}^{min}; es = 1....n_{es} \quad (4)$$

DG should maintain active and reactive power, Q_{dg} capacity constraints. For a particular interval, ramp-up, R_{dg}^{D} and ramp-down, R_{dg}^{U} constraints have to be followed considering initial active power, P_{dg}^{ini}

$$P_{dg}^{min} \leq P_{dg} \leq P_{dg}^{max}, and Q_{dg}^{min} \leq Q_{dg} \leq Q_{dg}^{max}; dg = 1....n_{dg} \quad (5)$$

$$P_{dg}^{inj} - R_{dg}^{D}\Delta t \leq P_{dg} \leq P_{dg}^{inj} + R_{dg}^{U}\Delta t \quad (6)$$

Similarly, BES has to maintain maximum charging power, P_{es}^{Cmax}, maximum discharging power, P_{es}^{Dmax}, and reactive power, Q_{ES} capacity constraints

$$P_{es}^{Cmax} \leq P_{es} \leq 0, and 0 \leq P_{es} \leq P_{es}^{Dmax}; es = 1...n_{es} \quad (7)$$

$$Q_{es}^{min} \leq Q_{es} \leq Q_{es}^{max}; es = 1...n_{es} \quad (8)$$

PV also has reactive power, Q_{PV} capacity constraints

$$Q_{pv}^{min} \leq Q_{pv} \leq Q_{pv}^{max}; pv = 1....n_{pv} \quad (9)$$

If network model is available, then node voltage constraints can be integrated considering sensitivity factor, $S_u^{V_{nv}}$ and voltage, V_{nv}^{ini} including the deviation of DER, Δu.

$$V_{nv}^{min} \leq V_{nv}^{ini} + \sum_{es=1}^{n_{es}} S_u^{V_{nv}}\Delta u \leq V_{nv}^{max}; nv = 1....n_{nv} \quad (10)$$

Here V_{nv}^{min} and V_{nv}^{max} are the minimum and maximum allowable voltage values in per unit. The high level flow chart

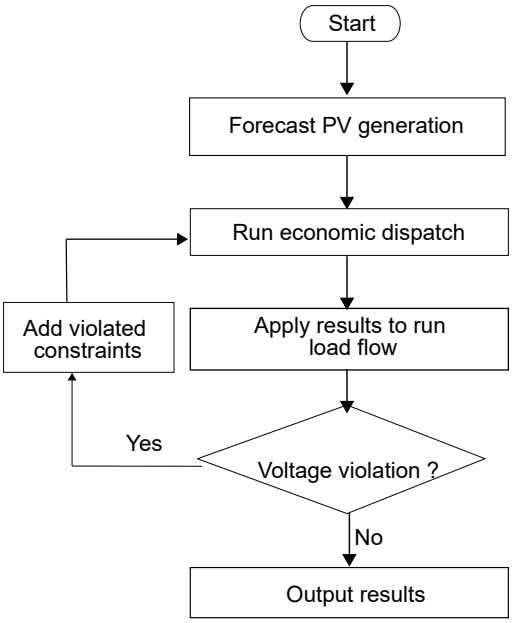

Fig. 2: Flow diagram of energy management system.

of network constraint grid edge EMS is shown in Figure 2. For each 15-minute interval, the LSTM based solar forecasting provides the estimated solar generation for the circuit segment in step 1. Economic dispatch is executed without considering the network constraints such as node voltage constraints in step 2. The optimization problem only considers equations (1)-(9). In step 3, control results are applied to the network model in OpenDSS to execute load flow. If no voltage violation is found in load flow, the economic dispatch result is the final control decision for the present time interval. If any voltage constraint violations are found, the corresponding voltage calculation equations i.e., equation (10), would be included in the optimization formulation as additional constraints in step 4. The modified optimization problem including equations (1)-(10) then solved again. The details of the energy management algorithm including network constraint is discussed in [7].

III. Real-Time Simulation Setup

For the real-time hardware-in-loop (HIL) simulation, circuit segment model is developed in Simulink and run in OPAL-RT real-time digital simulator. Load profiles are integrated in Simulink model as constant power sources. Three average inverter models are included in the circuit segment model to represent DERs in Simulink. The average model of the inverter is discussed in Section IVA. Four Raspberry Pi (RPi) controllers are utilized to communicate with DG, PV, BES and aggregated load. These RPis receive DER active and reactive power and load measurements from OPAL-RT simulator through IEC 61850 GOOSE communication protocol.

Data objects for DERs, loads and grid edge EMS are defined for complete information model following standard IEC 61850-7-420 Edition 2.0. These data objects are described in Section IVB. The data objects are mapped to IEC 61850 GOOSE publisher-subscriber messages by using libiec61850 protocol stack [9]. Conversion from IEC 61850 GOOSE protocol into Modbus communication protocol is done in RPis to get connected with the central controller where grid edge EMS runs in a separate RPi. Grid edge EMS sends the active and reactive power dispatch set points through Modbus communication after running the grid edge EMS described in Section II. An overview of the OPAL-RT, IEC 61850 models and GOOSE communication between four RPis, and Modbus communication with grid edge EMS in RPi setup is shown in Figure 3.

A. Inverter Model

In this work, a grid-following inverter control is implemented. A detailed mathematical model of the inverter is derived and used for obtaining gains of the primary controller. On top of the primary level controller, IEEE 1547-2018 compliant control functions for the reactive power support and voltage disturbance ride through are also developed.

Assuming inner current loop control bandwidth to be significantly lower than the resonant frequency (i.e neglecting the impact of the filter capacitor on the control loop), the voltage source control (VSC) can be modeled in a two-phase stationary reference frame as

$$L\frac{di_{ds}}{dt} + ri_{ds} = v_{g_{ds}} - v_{ds} \tag{11}$$

$$L\frac{di_{qs}}{dt} + ri_{qs} = v_{g_{qs}} - v_{qs} \tag{12}$$

$$C\frac{dv_{dc}}{dt} = \frac{3}{2v_{dc}}(i_{ds}v_{ds} + i_{qs}v_{qs}) - i_{dc} \tag{13}$$

Where L is the equivalent inductance $(L_f + L_g)$, L_f) is the converter side inductor, L_g is the grid side inductor, r is equivalent series resistance, v_{dc} is the dc bus voltage, C is the dc-link capacitor. The three-phase AC quantities are transformed into stationary wo-phase system, where i_{ds} and i_{qs} represents d and q axis components of the line current, v_{ds} and v_{qs} represents d and q axis components of the fundamental frequency component of the VSC AC voltages. The d and q axis components of the grid voltages in the stationary two-phase system are represented as $v_{g_{ds}}$ and $v_{g_{qs}}$, respectively.

The VSC control is implemented in the synchronously rotating frame, where the reference current tracking is achieved using the Proportional-Integral (PI) controller. The PI controller parameters are derived by setting the integral time constant of the PI controller equal to the time constant of the filter. The PI controller's proportional gain is derived to ensure technical optimum. For the BESS, the control block diagram is shown in Figure 4, where the current loop references are generated using the active and reactive power setpoints, derived from the secondary control. For the PV systems, the reference for the d-axis component of the current is derived using the outer DC bus voltage controller, as shown in Figure 5. The PI regulator gains of the outer DC bus voltage controller are derived using the symmetrical optimum.

As per the IEEE 1547-2018, the DERs are required to provide voltage regulation capability with the limit specified.

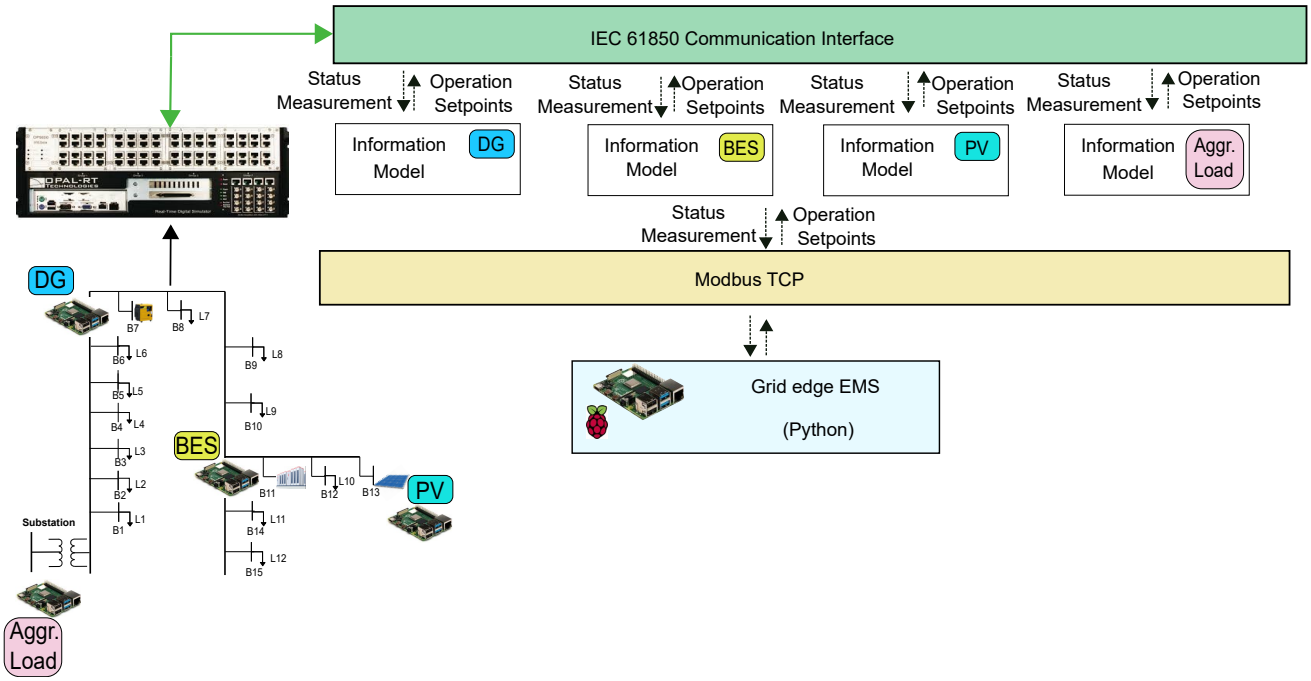

Fig. 3: Grid edge EMS real-time implementation set-up showing DERs interactions.

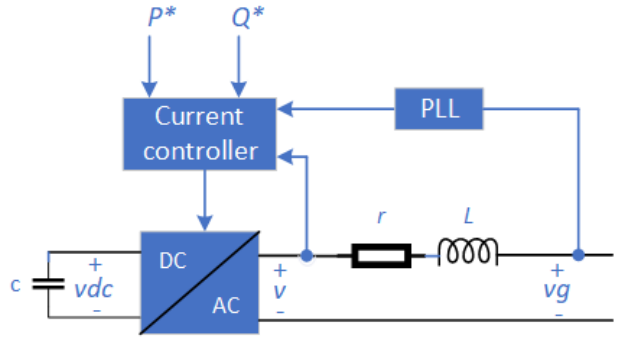

Fig. 4: Control block diagram of the battery energy management system.

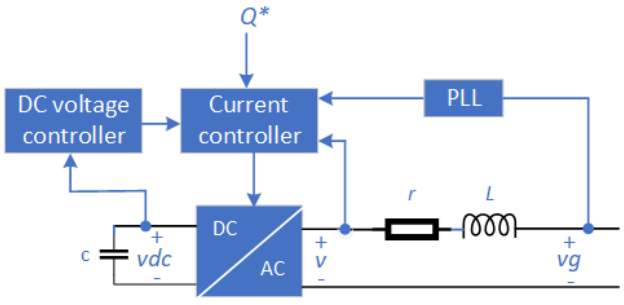

Fig. 5: Control block diagram of the photo-voltaic system.

They are also expected to respond to the abnormal grid conditions and ride through voltage and frequency disturbances. Operational requirements of the DERs based on IEEE 1547-2018 under normal and abnormal operating conditions, are also implemented in the developed models. The following operational modes under normal operating conditions are implemented:

(i) Voltage and reactive power control
- o Constant power factor mode
- o Voltage-reactive power mode
- o Active power – reactive power mode
- o Constant reactive power mode

(ii) Voltage and active power control
- o Constant active power mode
- o Voltage-active power mode

B. Information Model Development

To enable interoperability among different DERs and devices for the energy management use case, there is a need to define the type of data to be exchanged via standard exchangeable data objects as defined in IEC 61850-7-420 standard. A common method to achieve this is by adopting the Substation Configuration Language (SCL) [11]. SCL uses the XML to describe the intelligent electronic device (IED) information model including device capabilities, monitoring and control objects and its communication network. Description of the IED includes its configuration logical nodes, data objects and data attributes. SCL simplifies and automates the configuration of the information model, thus increasing the flexibility of information exchange between various actors and/or devices.

To create the SCL model, logical nodes (LN) and corresponding data objects (DO) for DER (e.g., PV unit, BES, DG) and loads are required to fulfill the information exchange. Table I provides the identified LN according to grid code operational functions for PV unit. Figure 6 reflects data exchange between LN class instances. These LNs are grouped into

TABLE I: Identified DER (PV Unit) LNs according to grid gode operational functions

Grid Code Operational Functions	IEC 61850-7-420 LNs
Disconnect/Connect Function	DGEN, DINV, DPVC, CSWI, XCBR/XSWI
Cease to Energize and Return to Service	DCTE
High/Low Voltage Ride-Through Function	DLVT, DHVT
High/Low Frequency Ride-Through Function	DLFT, DHFT
Frequency-Watt Function	DHFW, DLFW
Fixed (Constant) Power Factor Function	DFPF
Fixed (Constant) Reactive Power Function	DVAR
Volt-Var Control Function	DVVR

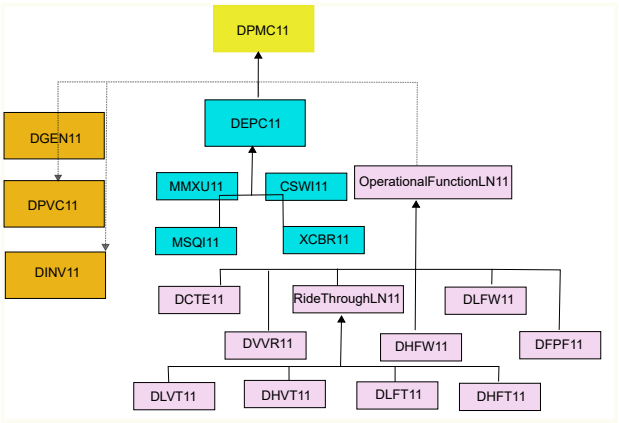

Fig. 6: Decomposition of DER (PV Unit) into IEC 61850-7-420 logical nodes.

multiple logical devices (LDs) so that the model is compatible with the DER recursive composition model defined in IEC 61850-7-420 standard. The DER resource for the case of a PV based system, shown in Figure 6, is modeled with the following LDs with corresponding identified LNs:

i) LD0 : The IED (LLN0, LPHD1)

ii) PMC : Power management control and operational functions (LLN0, DMPC11, DVVR11, DCTE11, DVVR11, DHVT11, DHFT11, DLFT11, DHFW11, DFPF11, DVAR11)

iii) ECP : Electrical connection point monitoring (LLN0, DECP11, MMXU11, XCBR11, CSWI11, MSQI11)

iv) GEN : Physical Equipment – Generator and PV array controller (LLN0, DGEN11, DINV11, DPVC11).

A sample XML code from ICD file defining various LDs is shown in Table II.

The aggregated load model includes power management (DPMC), load (DLOD) and electrical connection point (DECP) logical nodes for each individual load. The power management logical node (DPMC50) is used for load aggregation and includes references to the respective individual loads power management functions. Figure 7 shows data exchange between LN class instances for loads.

IV. Simulation Results and Analysis

For simulation, we have considered a circuit segment of a real distribution system feeder. One-line-diagram of the feeder is shown in Figure 8. One DG, one BES, and one PV are integrated in the feeder. The line-to-line voltage level is 12.47

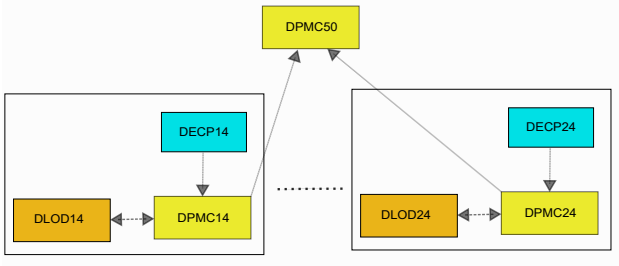

Fig. 7: Decomposition of load into IEC 61850-7-420 logical nodes.

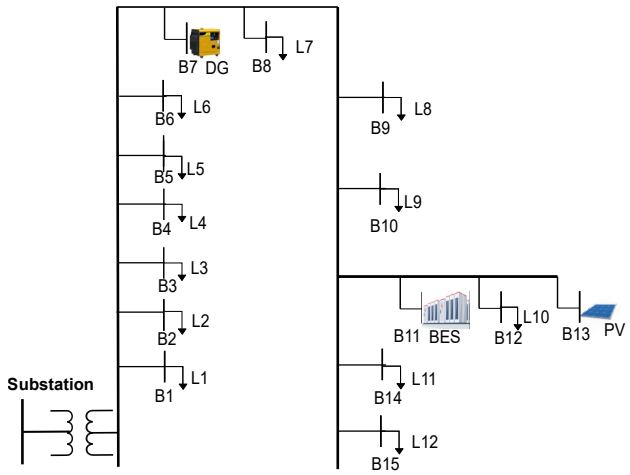

Fig. 8: One line diagram of a real distribution system circuit segment.

kV. The maximum load demand of the system is 14.5 MW. The prototype of network constraint grid edge EMS is developed in the Python environment. Python packages are utilized for both LSTM (Keras) and optimization (Ipopt). External function modules like OpenDSS for load flow is also exploited.

The DG is located at bus B7. Maximum capacity of DG is 3 MW and 0.4 MVAR. Ramp rate for DG is considered to be 3 MW/h. Fuel cost for DG is 0.1 $/kWh. Energy storage is located at bus B11. Maximum charging/discharging rate is considered as 200 kW. The charging and discharging efficiency of BES is 92%. Minimum and maximum SOC is chosen as 20% and 100%. The cost for BES is considered 0.16 $/kWhr to avoid discharge during off-peak hours. Maximum PV generation capacity is considered as 10 MW. Location of PV generator is on bus B13. PV generation for 24 hours with 15-min resolution is collected from [12]. In this distribution system, loads are provided in 12-nodes. Load data are extracted from [13] for these 12-nodes. The upper and lower bound for node voltages is followed by IEEE 1547-2018 where mandatory operating region is between 0.88 to 1.1 p.u [6].

The grid electricity purchase cost is considered the time-of-use (ToU) rate for summer days from Pacific Gas and Electric. The ToU is shown in Figure 9. It follows peak, partial-peak and off-peak hour rates. The peak hour electricity price is more than twice of the off-peak hour electricity price [14].

In real-time simulator, grid edge EMS is performed for a particular time instant 840th minute (1:00 PM) when solar

TABLE II: Sample code from IED capability decryption file (ICD)

Logical Device "ECP"

```
<LDevice inst="ECP">
   <LN0 inst="" lnClass="LLNO" lnType="DEMO_DER_LLNO_1" />
   <LN inst="1" lnClass="DECP" lnType="DEMO_DER_DECP_1" desc="Elctrical Connection Point" />
   <LN inst="1" lnClass="MMXU" lnType="DEMO_DER_EcpMMXU_1" prefix="Ecp" desc="Electrical Connection Point measurements" />
   <LN inst="1" lnClass="CSWI" lnType="DEMO_DER_EcpCSWI_1" prefix="Ecp" desc="Grid connection switch controller" />
   <LN inst="1" lnClass="XCBR" lnType="DEMO_DER_EcpXCBR_1" prefix="Ecp" desc="Grid connection breaker" />
</LDevice>
```

Logical Device "GEN"

```
<LDevice inst="GEN">
   <LN0 inst="" lnClass="LLNO" lnType="DEMO_DER_LLNO_1" />
   <LN inst="1" lnClass="DGEN" lnType="DEMO_DER_DGEN_1" desc="DER generating unit" />
   <LN inst="1" lnClass="DINV" lnType="DEMO_DER_DINV_1" desc="Inverter" />
   <LN inst="1" lnClass="DPVC" lnType="DEMO_DER_DPVC_1" desc="PVArray" />
</LDevice>
```

Logical Device "PMC"

```
<LDevice inst="PMC">
   <LN0 inst="" lnClass="LLNO" lnType="DEMO_DER_LLNO_1" />
   <LN inst="1" lnClass="DPMC" lnType="DEMO_DER_DPMC_1" desc="Power management controller" />
   <LN inst="1" lnClass="DFPF" lnType="DEMO_DER_DFPF_1" desc="Constant power doctor mode" />
   <LN inst="1" lnClass="DHFW" lnType="DEMO_DER_DHFW_1" desc="High-Freq Droop and Frequency Trip" />
   <LN inst="1" lnClass="DLFW" lnType="DEMO_DER_DLFW_1" desc="Low-Freq Droop and Frequency Trip" />
   <LN inst="1" lnClass="DVAR" lnType="DEMO_DER_DVAR_1" desc="Constant reactive power mode" />
   <LN inst="1" lnClass="DCTE" lnType="DEMO_DER_DCTE_1" desc="Constant reactive power mode" />
   <LN inst="1" lnClass="DVVR" lnType="DEMO_DER_DVVR_1" desc="Volt var mode" />
   <LN inst="1" lnClass="DHVT" lnType="DEMO_DER_DHVT_1" desc="HighVoltage Ride-through Events" />
   <LN inst="1" lnClass="DLVT" lnType="DEMO_DER_DLVT_1" desc="Volt var mode" />
   <LN inst="1" lnClass="DHFT" lnType="DEMO_DER_DHFT_1" desc="High Frequency Ride-through Events" />
   <LN inst="1" lnClass="DLFT" lnType="DEMO_DER_DLFT_1" desc="Low Frequency Ride-through Events" />
   <LN inst="1" lnClass="DWMX" lnType="DEMO_DER_DWMX_1" desc="Maximum active power mode" />
</LDevice>
```

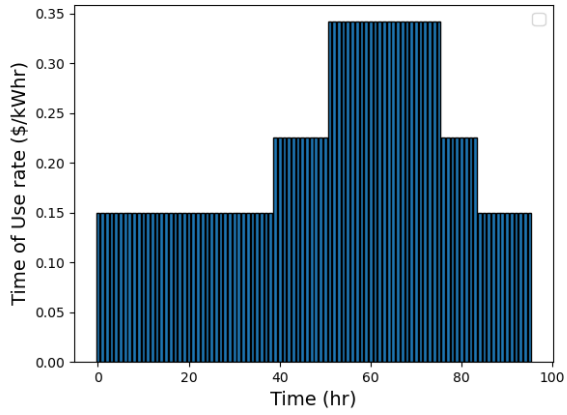

Fig. 9: Summer ToU rate from PG&E

generation is comparatively higher. Two economic dispatch algorithms are implemented to show the effectiveness of grid code compliant grid-edge EMS. The first algorithm runs economic dispatch without voltage constraint consideration. The snapshot of executing the algorithm in OPAL-RT is shown in Figure 10. It demonstrates that DERs are following the command from grid-edge EMS. Since maximum available PV generation is 10 MW at the time instant 840th minute, PV is scheduled to deliver this available 10 MW to reduce the overall electricity purchase cost. DG delivers 3 MW of power and BES reduces it's power injection from 0.5 MW to 0.2 MW. While running the following schedule, over voltage (>1.1 p.u.) is faced within 21 nodes in the system according to Figure 10 (a).

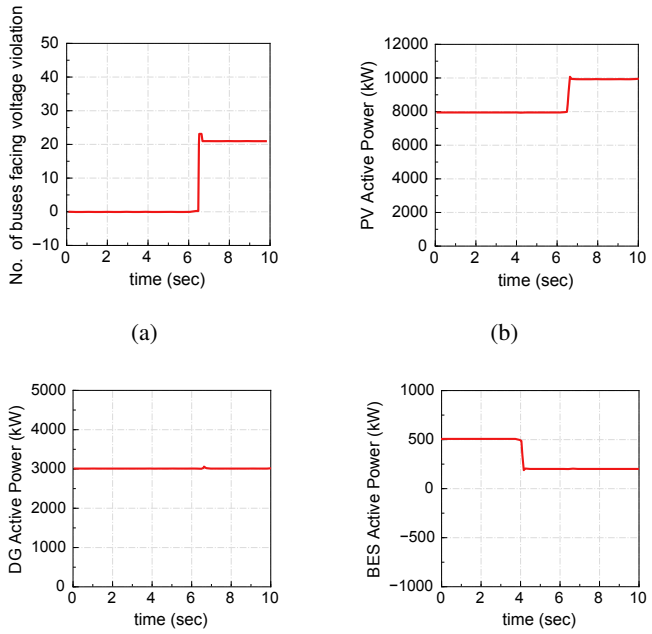

Fig. 10: Snapshot from OPAL-RT showing (a) number of buses facing violation, and active power set-points on (b) PV, (c) DG and (d) BES after the execution of grid edge EMS without considering voltage constraints.

Second algorithm includes voltage constraints in grid-edge EMS. To avoid voltage violation in the system, economic

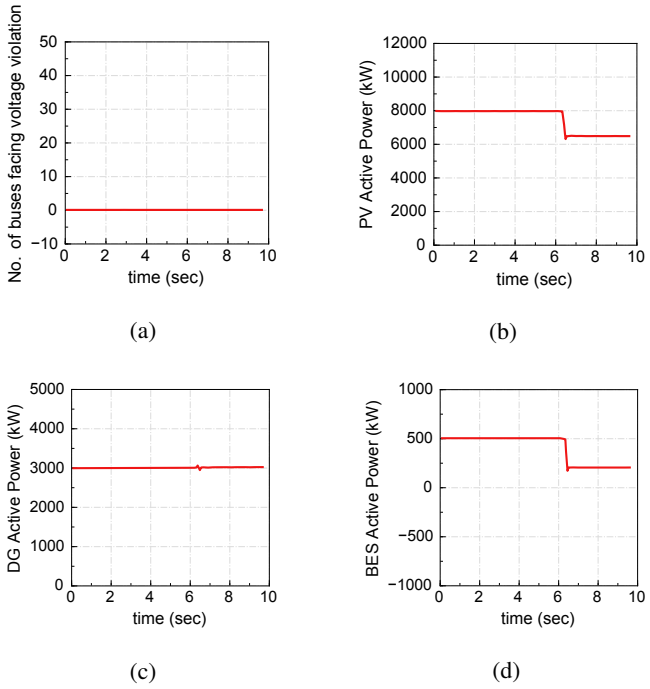

Fig. 11: Snapshot from OPAL-RT showing (a) number of buses facing violation, and active power set-points on (b) PV, (c) DG and (d) BES after the execution of grid edge EMS considering voltage constraints.

dispatch with violation constraints prefers to lower the active power generation usage of PV to 6.5 MW. The set-points sent from RPi for PV, DG and BES are captured from OPAL-RT snapshot and shown in Figure 11 (b), (c) and (d), respectively. Due to the lower injection of solar generation, there is no over voltage occurred in the modified distribution feeder. Figure 11 (a) depicts the number of buses facing voltage violation and execution of grid edge EMS schedules on OPAL-RT environment. It is portraying that following grid-edge EMS commands while violation constraints are considered, no voltage violation are seen in the overall system. The information received from IEC 61850 GOOSE interface of OPAL-RT through the information model in RPi for PV unit is shown in Figure 12. The values are converted into modbus information and sent to another RPi where grid-edge EMS is running. Grid-edge EMS reads DER status and load information through modbus communication from RPis and run EMS. A snapshot of grid-edge EMS execution and commands sent from RPi is shown in Figure 13. In RPi, grid edge EMS is termed as GEEMS.

V. Conclusion

The real-time simulation results shown in this work demonstrates significant performance of grid code compliant grid edge EMS by reducing the voltage violation on the overall circuit segment. Deployment of IEC 61850-7-420 DER information models and GOOSE communication protocol in real-time simulation portrays the benefits for utilization of advanced communication standards and protocol in EMS. This

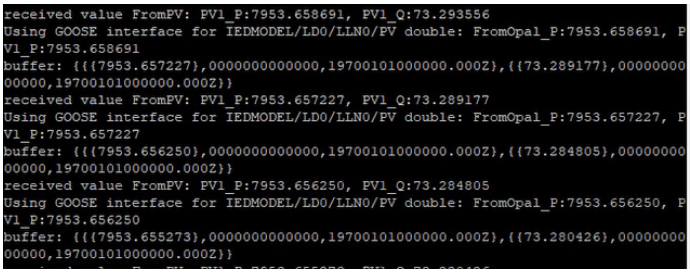

Fig. 12: Snap shot of PV measurements reading in RPi through GOOSE interface

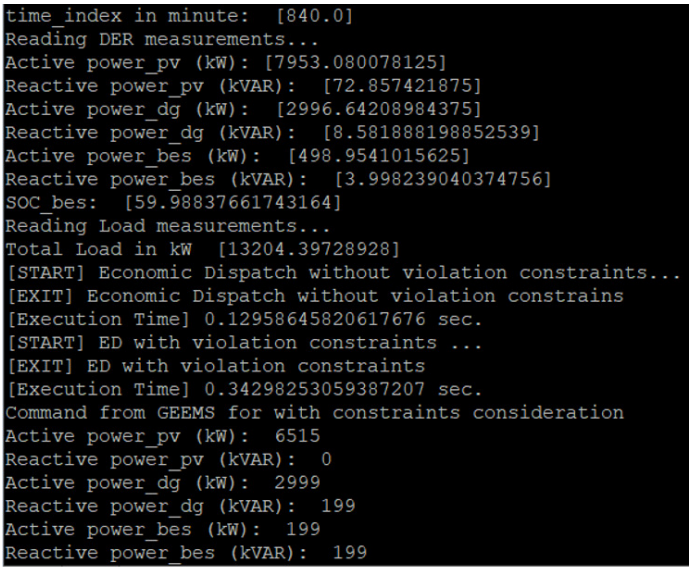

Fig. 13: Snap shot of grid edge EMS running in RPi

simplified DER integration improves interoperability. Overall, the proposed method and real-time implementation shows the reliability enhancement on grid edge technology.

VI. Acknowledgment

This work was supported by the Agency of the U.S. Government through the Department of Energy under Cooperative Agreement DE-OE0000896.

References

[1] M. F. Zia, E. Elbouchikhi, and M. Benbouzida, "Microgrids energy management systems: A critical review on methods, solutions, and prospects," *Applied Energy*, vol. 222, Jul. 2018.

[2] K. Mahmud, A. K. Sahoo, J. Ravishankar, and Z. Y. Dong, "Coordinated multilayer control for energy management of grid-connected ac microgrids," *IEEE Trans. on Ind. Applications*, vol. 55, no. 6, 2019.

[3] J. S. Girldo, J. A. Castrillon, J. C. López, M. J. Rider, and C. A. Castro, "Microgrids energy management using robust convex programming," *IEEE Trans. on Smart Grid*, vol. 10, no. 4, 2019.

[4] F. Bonassi, A. L. Bella, L. Fagiano, R. Scattolini, D. Zarrilli, P. Almaleck, and P. Sierra, "Software-in-the-loop testing of a distributed optimal scheduling strategy for microgrids' aggregators," in *Proc. 2020 IEEE PES Innovative Smart Grid Technologies Europe (ISGT-Europe)*. IEEE, 2020, pp. 1–6.

[5] F. Yang, X. Feng, and Z. Li, "Advanced microgrid energy management system for future sustainable and resilient power grid," *IEEE Trans. on Ind. Electronics*, vol. 55, no. 5, 2019.

[6] "IEEE standard for interconnection and interoperability of distributed energy resources with associated electric power systems interface," *IEEE Standard 1547-2018*, Feb. 2018.

[7] F. Hafiz, D. Ishchenko, and P. Almaleck, "Network constraints consideration for grid-edge energy management system," in *2022 IEEE PES Transmission and Distribution Conference Exposition*. IEEE, 2022, pp. 1–6.
[8] R. C. Dugan and D. Montenegro, "Reference guide. the open distribution system simulator (opendss)," *Electrical Power Research Institute, Inc,*, 2018.
[9] IEC 61850 and iec 60870-5-101/104 open source libraries. [Online]. Available: https://libiec61850.com/
[10] F. A. Gres, N. N. Schraudolph, and J. Schmidhuber, "Learning precise timing with lstm recurrent networks," *Journal of Machine Learning research*, vol. 3, no. 115-143, 2002.
[11] "IEC 61850-6 communication networks and systems for power utility automation part 6: Configuration de-scription language for communication in electrical substations related to ieds," *Edition 2.1*, 2018.
[12] Solar resource meteorological assessment project (solrmap). [Online]. Available: http://www.nrel.gov/midc/lmu/
[13] (2021) Load data. [Online]. Available: http://wzy.ece.iastate.edu/Testsystem.html
[14] (2020) Time of use rates. [Online]. Available: http://www.pge.com